encit 2020

ABCM Associação Brasileira de Engenharia e Ciências Mecânicas

18th Brazilian Congress of Thermal Sciences and Engineering
November 16-20, 2020 (Online)

ENC2020-0460
THE EFFECT OF THE SMAGORINSKY CONSTANT ON LES OF COAXIAL TURBULENT JETS

Jean Monteiro de Pinho
IFSC, Federal Institute of Santa Catarina, Euclides Hack St, 1603, 89820-000, Xanxerê, SC, Brazil
jean.pinho@ifsc.edu.br

André Rodrigues Muniz
UFRGS, Department of Chemical Engineering, Rua Engenheiro Luiz Englert, s/n, 90040-040, Porto Alegre, RS, Brazil
munizeq@gmail.com

Abstract. *Large Eddy Simulation (LES) is an efficient technique to simulate turbulent flows of practical interest, based on the elimination of flow scales smaller than a characteristic length and direct resolution of the largest scales. The effect of subgrid-scales is often described by a subgrid viscosity, also called eddy viscosity. The Smagorinsky subgrid model is frequently used to describe the eddy viscosity in the literature, presenting good results for a variety of flows. However, the use of this model requires the choice of a value for the Smagorinsky constant, which has no universal value, and depends on characteristics of the flow and even on details of the numerical solver. In this work, we studied the effect of the Smagorinsky constant used in the LES of turbulent coaxial jets using a GPU-based solver called PMLES, comparing the results with experimental data available in the literature. Our results demonstrate that the use of inadequate values of this constant, even within the range recommended by the literature, can result in simulations that are far from reality.*

Keywords: *Subgrid Scale Models, LES, Numerical Simulation, Jets, Turbulence*

1. INTRODUCTION

Turbulence is a phenomenon present in most flows observed in nature and in engineering applications. Turbulent flows are unstable and their properties exhibit fluctuations that are time and space dependent. One of the most striking features of turbulent flows is the multiplicity of scales. They are present from the largest structures (low frequencies), which are controlled by the geometry of the flow, to the smallest structures (high frequencies), which are controlled by molecular viscosity. The numerical simulation of turbulent flows remains a challenge in computational fluid dynamics (CFD). In this sense, intense research has been made toward understanding and controlling turbulence, due to its importance in a wide variety of engineering applications, such as in aerodynamics, engines, industrial equipment and others.

The Large Eddy Simulation (LES) is a efficient technique to simulate turbulent flows, based on the elimination of all scales of the flow smaller than a characteristic length scale Δ. The separation of the scales is performed through the proper application of a low-pass filter in the system of equations, as discussed in the next section. The filtering operations result in the so called LES equations, able to describe the flow in the largest scales (Lesieur *et al.*, 2005). In terms of computational cost, LES is an intermediate methodology between the other traditionally used in simualtion of turbulent flows (DNS and RANS). It allows to capture the anisotropic turbulence that occurs in the large scales through the solution of the intermediate scales, while the small scales are described by homogeneous isotropic turbulence models.

In the framework of LES, there are many sub-models for describe the dissipative effect of small scales. The studies of Piomelli (1999), Lesieur *et al.* (2005) and Sagaut (2006) discuss these models in detail. The most commonly used is the Smagorinsky Model (Smagorinsky, 1963), based on the concept of turbulent viscosity proposed by Boussinesq. The utilization of the Smagorinsky subgrid model requires setting the value of an *ad hoc* constant, called *Smagorinsky constant* C_s. There is no consensus in the literature on the adequate value of this constant. For developed flow with homogeneous and isotropic turbulence the theoretical value of C_s is 0.18 (Pope, 2000; Sagaut, 2006). In the case of tubulent jets Ilyushin and Krasinsky (2006) used $C_s = 0.17$, as suggested by Pope (2000); Wilson and Demuren (1997), and Jones *et al.* (2002) used 0.10-0.12 as suggested by Lesieur *et al.* (2005) while Deardorff (1970), McMillan (1980) and Ferziger and Peric (2012) use C_s between 0.06-0.10. According to Ilyushin and Krasinsky (2006) and Brès and Lele (2019) the adequate value of the Smagorinsky constant, C_s is not universal, and depends on the numerical dissipative characteristics of the solver.

In this sense, the objective of this work is to carry out an analysis of the impact of the Smagorinsky constant in the LES of a coaxial turbulent jet, and determine the appropriate value to be used in the PMLES (Pinho and Muniz, 2020)

solver, a computational tool designed specifically to run on hybrid architectures CPU-GPU.

2. METHODOLOGY

2.1 LES Modeling

In the LES methodology, the filtering operation is responsible to separate mathematically a variable $f(\mathbf{x},t)$ in two components: one related to the large scales of the flow to be solved $\overline{f}(\mathbf{x},t)$ and other to the small scales to be modeled $f'(\mathbf{x},t)$ (also called subgrid scales):

$$f(\mathbf{x},t) = \overline{f}(\mathbf{x},t) + f'(\mathbf{x},t) \tag{1}$$

This approach is also known as Leonard decomposition (Pope (2000)). The filtering consists of the convolution of the variable to be filtered on the filter function G

$$\overline{f}(\mathbf{x},t) = \int_D f(\mathbf{x}',t)G(\mathbf{x}-\mathbf{x}':t)d\mathbf{x} \tag{2}$$

where *D* is the domain on which the operation must be performed.

The filtering process aims to eliminate or smooth out fluctuations that are smaller than the predefined cutoff wave number. The challenge is to find a good balance between filter size, accuracy and computational cost. LES modeling involves two filtering processes: : *i*) a dimensional filter (δ) and *ii*) a grid filter (Δ) (Kuo and Acharya, 2012). The phenomena that occurs in a scale smaller than the grid filter cannot be captured by any of the filters, and they are always modeled. The scales smaller than grid filter (Δ) are called sub-grid scales.

The Large Eddy Simulation modeling allows using either explicit or implicit filters, provided that they represent the properties of the sub-grid terms. Most applications in LES use the constant volumetric filter, also called top-hat filter (Silva Freire *et al.*, 2002)

$$G(\mathbf{x}) = \begin{cases} 1/\Delta^3, \text{se } |x_i| \leq \Delta/2, \quad i=1,2,3; \\ 0, \text{otherwise}, \end{cases} \tag{3}$$

which is an implicit filter, considering that the characteristic size of the filter is equal to the mesh spacing length. In this case the filtering and differentiation operation commute. This approach is also called Schumann filtering (Huai, 2006) and was used in this work.

In the present work, Favre averaging was applied to the conservation equations. A filtered variable f is defined as:

$$\widetilde{f} = \frac{\overline{\rho f}}{\overline{\rho}}, \tag{4}$$

and the following relations are verified Kuo and Acharya (2012):

$$\overline{\rho u_i} = \overline{\rho}\widetilde{u_i}, \tag{5}$$

$$\overline{\rho u_i u_j} = \overline{\rho}\widetilde{u_i u_j}. \tag{6}$$

A variable can be then decomposed into its Favre filtered component $\widetilde{f}$ and its subgrid component f':

$$f(\mathbf{x},t) = \widetilde{f}(\mathbf{x},t) + f'(\mathbf{x},t). \tag{7}$$

This procedure can be applied to velocity. Variables whose effects of the density are inherent to the measurement process, such as pressure, stress tensors and the specific mass itself, do not need to be filtered by the Favre average. For these variables, the conventional time averaging can be used (Kuo and Acharya, 2012).

As a result of the filtering process, the momentum equation becomes

$$\frac{\partial(\overline{\rho u_i})}{\partial t} + \frac{\partial(\overline{\rho u_i u_j})}{\partial x_j} = \frac{\partial \overline{p}}{\partial x_i} + \mu\left(\frac{\partial^2 \overline{u_i}}{\partial {x_j}^2} + \frac{\partial^2 \overline{u_j}}{\partial {x_i}^2}\right) \tag{8}$$

Details of the application of the filter in the momentum equation can be seen in Moint *et al.* (Moin *et al.*, 1991) and Kuo and Acharya (Kuo and Acharya, 2012).

The nonlinear term of the filtered equation (Eq. 8) resulted in a product of two filtered variables, making their solution unfeasible. This nonlinear term can be treated using the Leonard decomposition in terms of the Favre filter (Sagaut, 2006), defined in Eq. 1 and Eq. 4, so that

$$\overline{\rho u_i u_j} \equiv \overline{\overline{\rho}(\widetilde{u_i} + {u_i}')(\widetilde{u_j} + {u_j}')}$$

$$\overline{\rho u_i u_j} = \overline{\rho}\widetilde{u_i}\widetilde{u_j} + \overline{\rho}\widetilde{u_i}\overline{{u_j}'} + \overline{\rho {u_i}'}\widetilde{u_j} + \overline{\rho {u_i}' {u_j}'}. \tag{9}$$

Adding and subtracting the term $\overline{\rho}\widetilde{u_i}\widetilde{u_j}$ and replacing in the Eq. 8 we have

$$\frac{\partial\left(\overline{\rho u_i}\right)}{\partial t}+\frac{\partial\left(\overline{\rho}\widetilde{u_i}\widetilde{u_j}\right)}{\partial x_j} = \frac{\partial\overline{p}}{\partial x_i}+\mu\left(\frac{\partial^2\widetilde{u_i}}{\partial {x_j}^2}+\frac{\partial^2\widetilde{u_j}}{\partial {x_i}^2}\right)-\frac{\partial}{\partial x_j}\left[\overline{\rho\widetilde{u_i}\widetilde{u_j}}-\overline{\rho}\widetilde{u_i}\widetilde{u_j}+\overline{\rho\widetilde{u_i}u_j{}'}+\overline{\rho u_i{}'\widetilde{u_j}}+\overline{\rho u_i{}'u_j{}'}\right]. \quad (10)$$

The subgrid-scale stress tensor is defined as $(\sigma_{ij})_{sgs}$, as

$$(\sigma_{ij})_{sgs} = \overline{\rho u_i u_j}-\overline{\rho}\widetilde{u_i}\widetilde{u_j} \quad (11)$$

$$(\sigma_{ij})_{sgs} = \overline{\rho}\left(\widetilde{u_i u_j}-\widetilde{u_i}\widetilde{u_j}\right), \quad (12)$$

$$(\sigma_{ij})_{sgs} = \overline{\rho\widetilde{u_i}\widetilde{u_j}}-\overline{\rho}\widetilde{u_i}\widetilde{u_j}+\overline{\rho}\left(\overline{\widetilde{u_i}u_j{}'}+\overline{u_i{}'\widetilde{u_j}}\right)+\overline{\rho u_i{}'u_j{}'}$$

$$(\sigma_{ij})_{sgs} = L_{i,j}+C_{i,j}+R_{i,j} \quad (13)$$

where $L_{i,j}$ is the Leonard-stress tensor that represents the interaction between the resolved scales, that result in the subgrid contributions: $C_{i,j}$, the Cross-stress tensor that represents the interaction between the resolved scales and the unresolved scales, and $R_{i,j}$, the Reynolds-stress tensor that represents the interaction between the unresolved small scales. The conservation equations can be then written as follows:

$$\frac{\partial\overline{\rho}}{\partial t}+\frac{\partial\overline{\rho}\widetilde{u_i}}{\partial x_i} = 0; \quad (14)$$

$$\frac{\partial\left(\overline{\rho}\widetilde{u_i}\right)}{\partial t}+\frac{\partial\left(\overline{\rho}\widetilde{u_i}\widetilde{u_j}\right)}{\partial x_j} = -\frac{\partial\overline{p}}{\partial x_i}+\frac{\partial(\sigma_{ij})_{sgs}}{\partial x_i}+\frac{1}{Re}\left(\frac{\partial^2\widetilde{u_i}}{\partial {x_j}^2}+\frac{\partial^2\widetilde{u_j}}{\partial {x_i}^2}\right). \quad (15)$$

2.2 Smagorinsky Subgrid Model

The Smagorinsky subgrid model (Smagorinsky, 1963), is based on the concept of turbulent viscosity proposed by Boussinesq. The eddy viscosity concept is based on the hypothesis that the energy transfer mechanism of the scales solved to the subgrid scales is analogous to the molecular momentum transfer mechanism, represented by the diffusive term with the viscosity μ. According to this principle, the subgrid stress tensor can be described as:

$$\sigma_{ij}^{sgs} = -\nu_t\left(\frac{\partial\widetilde{u_i}}{\partial x_j}+\frac{\partial\widetilde{u_j}}{\partial x_i}\right)+\frac{2}{3}\nu_t\frac{\partial\widetilde{u_k}}{\partial x_k}\delta_{ij}, \quad (16)$$

The use of the subgrid stress tensor as defined in Eq.16 allows us to combine the eddy viscosity μ_t with the molecular viscosity, resulting in a dimensionless effective viscosity μ_e:

$$\mu_e = \frac{\mu+\mu_t}{\mu}, \quad (17)$$

Then, the Eq. 15 can be rewritten as

$$\frac{\partial\left(\overline{\rho}\widetilde{u_i}\right)}{\partial t}+\frac{\partial\left(\overline{\rho}\widetilde{u_i}\widetilde{u_j}\right)}{\partial x_j} = -\frac{\partial\overline{p}}{\partial x_i}+\frac{\mu_e}{Re}\left(\frac{\partial^2\widetilde{u_i}}{\partial {x_j}^2}+\frac{\partial^2\widetilde{u_j}}{\partial {x_i}^2}\right). \quad (18)$$

The turbulent viscosity model proposed by Smagorinsky (Smagorinsky, 1963) was developed assuming that the eddy viscosity (μ_t) is proportional to the characteristic length of the filter Δ, and to the characteristic subgrid velocity v_Δ, that are defined as

$$v_\Delta = \Delta|\bar{S}| \quad (19)$$

$$\Delta = \sqrt[3]{\Delta x\Delta y\Delta z}, \quad (20)$$

where the norm $|\bar{S}|$ is calculated from the second invariant of strain rate tensor.

$$|\bar{S}| = \sqrt{2\bar{S}_{ij}\bar{S}_{ij}}, \quad (21)$$

Then, the turbulent viscosity is evaluated as

$$\mu_t = \rho(C_s\Delta)^2|\bar{S}|, \quad (22)$$

where C_s is called the Smagorinsky constant, whose effect of using different values for it is investigated in this work. We can see that the turbulent viscosity has a quadratic dependence on C_s; large values of C_s may then introduce significant dissipation on the model, being able to smooth out the turbulence due to an excess of dissipation of the turbulent kinetic energy in the small scales modeled. On the other hand, a small value for C_s makes the solution procedure unstable, considering that the turbulent kinetic energy produced at large scales and transported to the small scales is dissipated at a lower rate than it is being generated. Consequently, the hypothesis of local equilibrium of turbulent kinetic energy, for larger scales than the dissipative scale of Kolmogorov, is not respected (Hällqvist, 2006).

2.3 Numerical Details

Details of code implementation and numerical methodology are presented in the introductory paper of PMLES (Pinho and Muniz, 2020). The PMLES solver was developed for running LES in mixed architectures employing GPU (graphic processing units) computing, which has becoming more popular in LES (Markesteijn and Karabasov, 2018; Terrana *et al.*, 2020).

In summary, the filtered equations (Eq. 18) are discretized by the finite difference method, using second-order schemes and a regular three-dimensional structured cartesian grid with uniform spacing. The use of a regularly spaced grids avoids the propagation of errors due to filter size variations (Piomelli, 1999; Ilyushin and Krasinsky, 2006). Temporal discretization was performed using a three-stage second-order Runge-Kutta scheme Blazek (2015), with a dimensionless time step of Δt is 1.75×10^{-4}, which ensures CFL stability. We should note that use of an explicit scheme is quite efficient when working on a SIMT (*Single Instruction Multiple Thread*) architecture of GPU cards (Quadros, 2016), because it enables a massively parallel execution of thousands of threads independently and simultaneously (Ruetsch and Fatica, 2011). The pressure field for the incompressible flow is computed using the SOLA (SOLution Algorithm) method (Hirt *et al.*, 1975; Wilson *et al.*, 1988; Fortuna, 2000).

The implementation was performed using CUDA Fortran programming to run on a single workstation properly prepared. The Figure 1 presents the flowchart of the PMLES solver, where we can see that the control of the execution flow is done by the host (blue box), which can also execute subprograms and functions, while parts of code are executed by the GPU (device - green box). Pinho and Muniz (2020) report that with this hybrid implementation are possible *speedup* of order of 55.

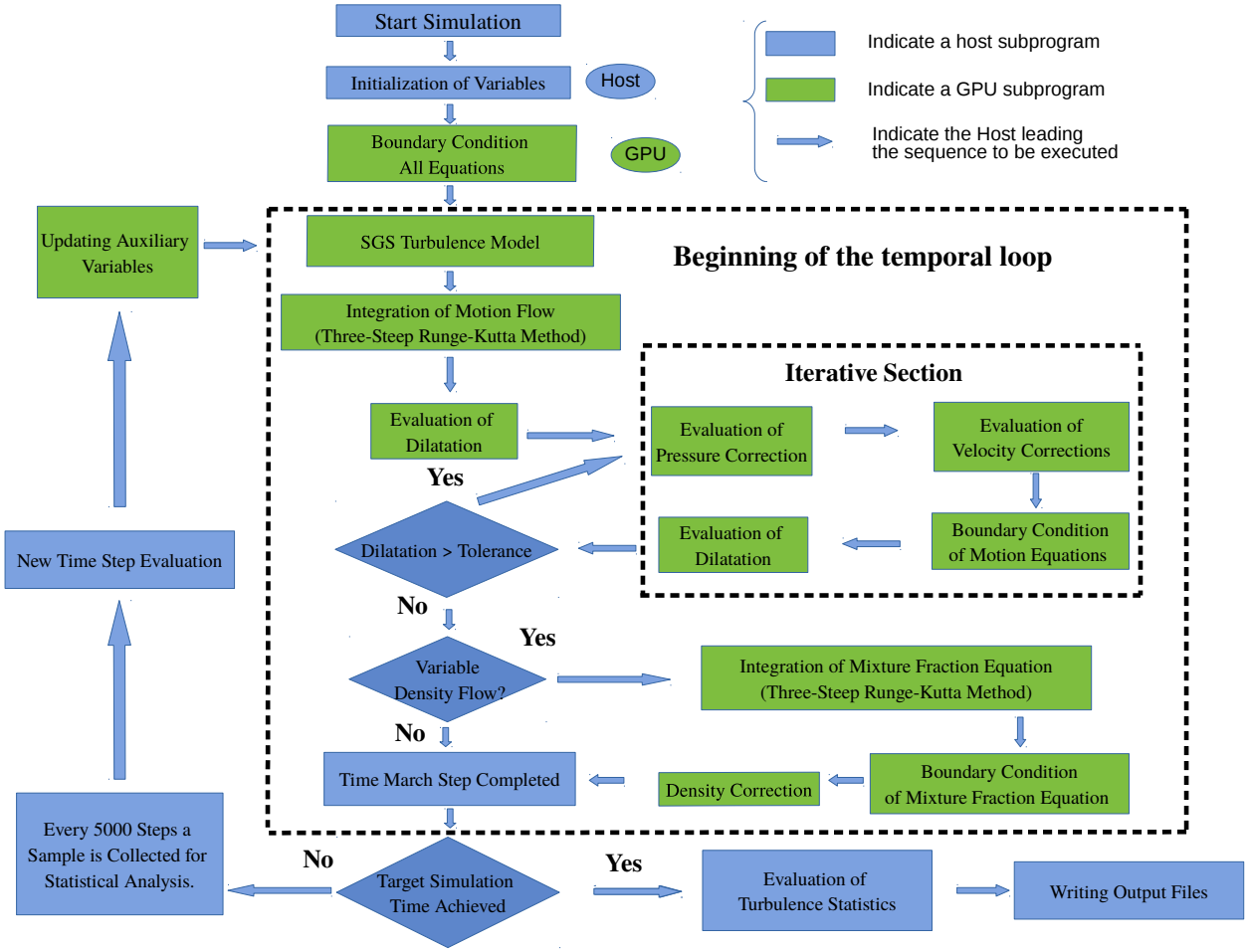

Figure 1. PMLES Solver Flowchart

2.4 Description of the test problem

To carry out the analysis, we chose the turbulent coaxial round jet described in Amielh *et al.* (1996) and Djeridane *et al.* (1996). A schematic description of the geometry of the experimental apparatus is shown in Fig. 2. The domain consists in a rectangular duct section with a circular coaxial duct for the high velocity fluid injection. Air at standard conditions

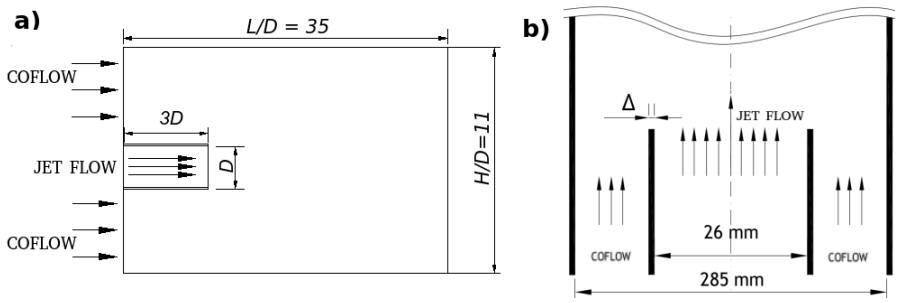

Figure 2. (a) Computational domain of the test problem and characteristic dimensions. (b) Characteristic dimensions and velocities ate the nozzle.

flows in both ducts. The original setup has dimensions $L/D \simeq 50$ and $H/D \simeq 11$. Due to the high computational cost of the full problem, and considering that the analysis is focused on the near field, the length of computational domain was reduced to $L/D = 35$.

The computational domain was discretized using $N_x = 1004$ and $N_z = N_y = 317$ points, resulting on a regular mesh spacing of 3.49×10^{-2} and a domain with $\sim 1 \times 10^8$ cells. Despite using a Cartesian mesh, the circular injection duct of the jet was relatively well modeled. The momentum flux deviation by the cubic cells was evaluated and remained below 1 %.

The jet properties as defined in Fig. 2 are the same as in the experimental works Amielh *et al.* (1996); Djeridane *et al.* (1996) (inlet jet velocity $U_j = 12\ m/s$, and coflow velocity $U_{coflow} = 0.09\ m/s$, resulting in a Reynolds jet number of $Re = \frac{\rho U_j D}{\mu} = 20650$). The inlet boundaries and the rigid boundary walls (far from the regions of interest) are modeled by Dirichlet conditions, and a Neumann boundary condition for fully developed flows was applied at the outlet, assuming that the gradient of normal momentum flux is null. For the inlet jet zone, a fully developed velocity profile for circular duct Abramovich (1963) was set:

$$\frac{\widetilde{u}\,(r)}{\widetilde{u}_{max}} = \left(1 - \frac{r}{R}\right)^{1/7}. \tag{23}$$

For the coflow zone, a planar velocity profile was defined. In both inlet zones, the velocity fluctuations were not included.

3. RESULTS

The turbulent flow in the coaxial jet described in the previous section was simulated by LES with the Smagorinsky eddy viscosity model using for the constant C_s values from 0.050 to 0.095. A comparison of results was done using profiles of time-averaged variables in the central plane (2D) and along the main axis and selected cross sections (1D). The variables used in the analysis were the dimensionless velocity U_{adm} and the dimensionless turbulence intensity $u^{'}{}_{adm}$, defined as

$$U_{adm} = (U_L - U_{coflow})/(U_j - U_{coflow}), \tag{24}$$

$$u^{'}{}_{adm} = u^{'}{}_{rms}/\,(U_L - U_{coflow}) \tag{25}$$

where U_L is the local axial component of average velocity and u'_{rms} the root mean square velocity. These are computed by

$$U_L = \frac{\sum_{a=1}^{N} u_a}{N} \tag{26}$$

$$u'_{rms} = \sqrt{\frac{\sum_{a=1}^{N} \left(u_a - \langle\langle u \rangle\rangle\right)^2}{N}} \tag{27}$$

where u_a is a sample of the axial instantaneous velocity on a given point of the domain. The average values were calculated over $N = 300$ samples taken every 10000 steps of time after the steady regime is reached.

Representative results of these simulations are shown in Figure 3, which presents the field of U_L, μ_e and u'_{rms} in the central plane of the domain, predicted by the Smagorinsky model with $C_s = 0.060$. In general, the structure of the jet velocity field was well predicted, in agreement with the expected theoretical structure described in previous works Lipari and Stansby (2011). This result is very useful for a qualitative analysis, but one dimensional profiles are more suitable for quantitative comparisons between the effect of using different values for C_s, as done below.

As discussed in Sec. 1, a wide range of values for this constant has been used in the previous literature ($0.055 - 0.170$). We started with values for the constant C_s in the range of $0.100 - 0.120$ as suggested before Kuo and Acharya (2012).

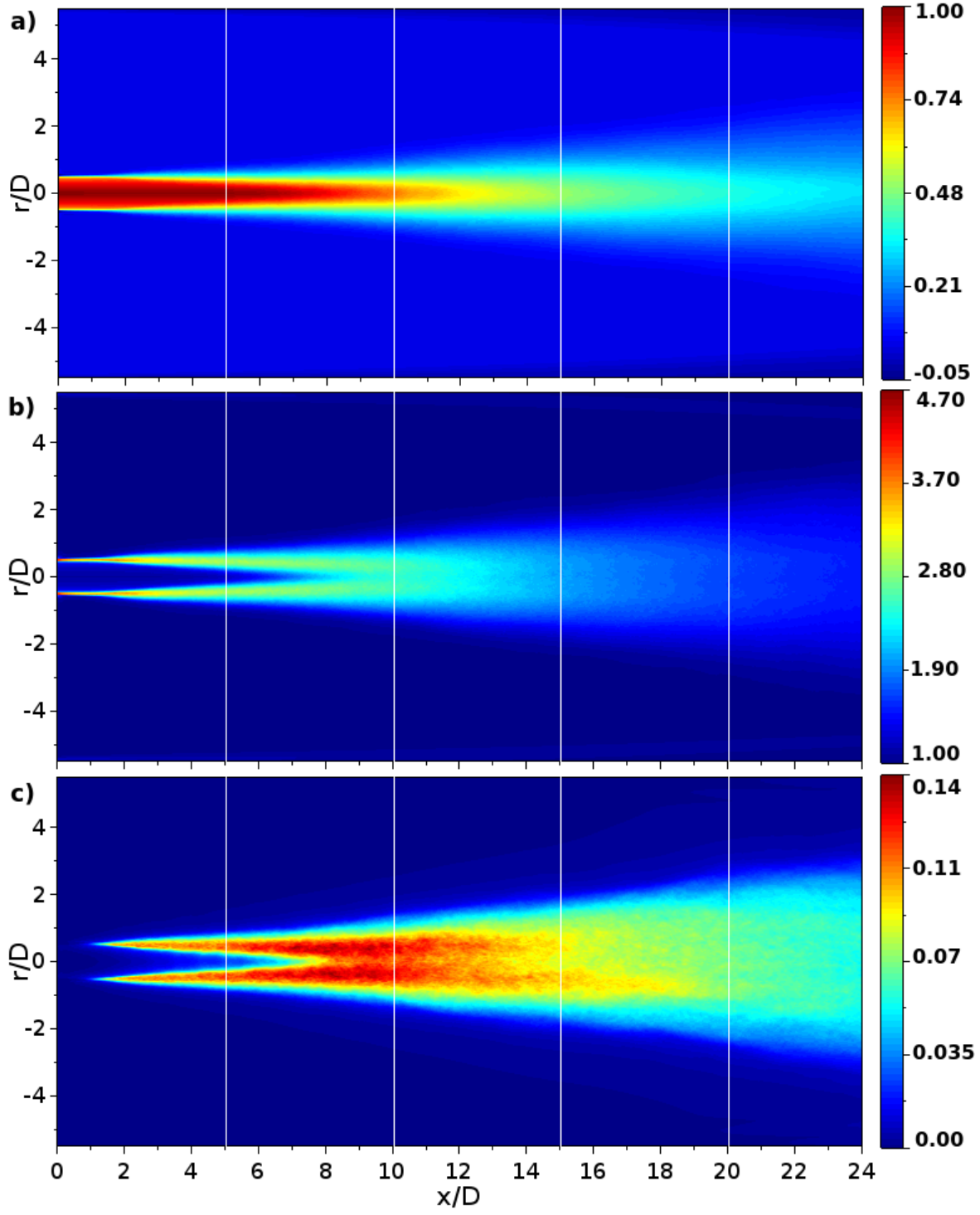

Figure 3. Average fields computed by Smagorinsky subgrid model using $C_s = 0.060$ for a)U_L , b) μ_e and c) u'_{rms}.

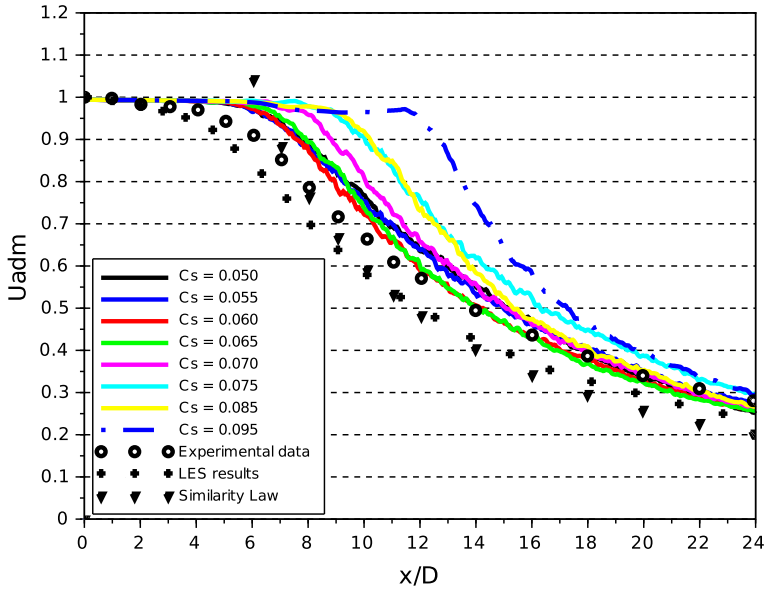

Figure 4. Profiles for dimensionless velocity U_{adm} along the main axis, obtained with the Smagorinsky model for varied values of C_s, compared to literature data Amielh *et al.* (1996); Wang *et al.* (2008); Chen and Rodi (1980).

However, we found that the Kelvin-Helmholtz instabilities, responsible for the first vortices, were quickly dissipated after the inlet zone. In order to reduce the dissipative effect of the model, the range of C_s used was reduced to $0.050 - 0.095$, which are close to the minimum values recommended in the literature Ferziger and Peric (2012).

Figure 4 presents the results obtained for the axial profile of the dimensionless velocity U_{adm} according to the Smagorinsky model using eight values of C_s within the aforementioned range. For comparison purposes, we included in the same plot the experimental data reported by Amielh *et al.* (1996), the numerical results obtained by LES from Wang *et al.* (2008) and the result obtained by the Similarity Law of Chen and Rodi (1980). These differ from each other, but exhibit a reasonable agreement with respect to observed trends and length of the relevant zones.

The results of Fig. 4 show that the curves for $C_s \leq 0.065$ practically coincide. This behavior indicates that the sensitivity of the Smagorinsky model is small for $C_s < 0.070$ with respect to this variable. For $C_s > 0.075$ the subgrid stress tensor becomes very dissipative, and the transition to turbulence occurs further from the nozzle, distorting the jet physics. The computed profiles show a very good agreement with the experimental results Amielh *et al.* (1996) in regions far from the inlet, but a delay on the transition to turbulence is clearly observed. We can note that although there is a delay in the transition to turbulence, the deviations in the obtained results are in the same order as deviations obtained in the work of Wang *et al.* (2008) and by the Similarity Law Chen and Rodi (1980). We think that this delay may be due to the boundary condition used for the inlet regions (without the presence of turbulent fluctuations). The effect of modeling of the inlet boundary condition in this problem will be subject of future works.

Figure 5 shows the profile of the dimensionless turbulence intensity u'_{adm} along the main axis. The profiles obtained in the simulations are qualitatively very similar to the experimental one (as if they were displaced vertically downwards). An interesting point is that this downward displacement has the same order of magnitude of the intensity of turbulence existing in the flow of the experimental jet ($\sim 4\%$) Amielh *et al.* (1996), which was not taken into account in the inlet boundary condition as mentioned before. After the end of the potential region, we observe a marked reduction in the deviation between u'_{adm} calculated with respect to the experimental data, which remains below 10%. The best results were obtained for values of C_s of 0.060 and 0.065, while the biggest deviations 0.070 and 0.075, due to the extension of the jet potential cone.

Given these results, the most adequate value of C_s was chosen through the evaluation of the mean squared errors of the computed average dimensionless axial component of velocity (MSE1) and turbulence intensity (MSE2) with respect to the experimental data Amielh *et al.* (1996), defined as

$$MSE1\left(\widehat{U_{adm}}\right) = \frac{1}{N}\sum_{a=1}^{N}\left[\left(\widehat{U_{adm}}\right)_a - \left(U_{adm}\right)_a\right]^2 \tag{28}$$

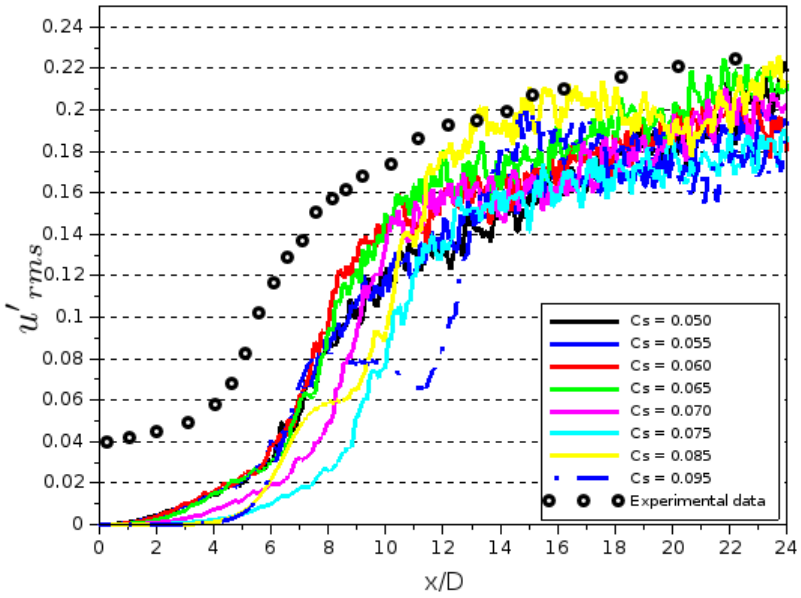

Figure 5. Profiles for dimensionless turbulence intensity u'_{adm} along the main axis, obtained with the Smagorinsky model for varied values of C_s, compared to literature data Amielh *et al.* (1996).

$$MSE2\left(\widehat{u'_{adm}}\right) = \frac{1}{N}\sum_{a=1}^{N}\left[\left(\widehat{u'_{adm}}\right)_a - \left(u'_{adm}\right)_a\right]^2. \tag{29}$$

Table 1 shows the computed MSE1 and MSE2 for simulations using the eight tested values for C_s. The lowest errors were found for $C_s = 0.060$. Therefore, this is the value of the constant C_s that produces the best results for the studied problem.

Table 1. Comparison between the mean squared errors produced using different values of the Smagorinsky constant C_s.

C_s	**MSE1**($\times 10^3$)	**MSE2**($\times 10^3$)
0.050	3.24	3.38
0.055	2.87	3.05
0.060	1.65	2.31
0.065	2.77	2.48
0.070	6.47	4.14
0.075	15.10	6.31
0.085	14.60	4.03
0.095	30.20	4.61

4. CONCLUSIONS

The main objective of this work was to evaluate the effect of utilization different values for the Smagorinsky constant in LES of a coaxial turbulent jet. Simulations were performed using a range of C_s values of $0.050 - 0.095$ and results were compared to experimental data and other numerical results from the literature. The results showed that $C_s = 0.060$ led to the smallest deviations for the average velocities with respect to the experimental data. To reach this quality of results, the constant C_s was "optimized" for the coaxial turbulent jet solution. This calibration was not trivial as it seems, since the range of C_s recommended in the literature is quite wide. Since the use of values for C_s not adequate to the numerical characteristics of the solver can distort the physics of the problem under study, we think that this result might motivate further studies on the use of the Smagorinsky subgrid model in similar systematic studies for various problems, but using the same numerical arrangement, the same description of the boundary condition and preferably the same solver, as suggested by Brès and Lele (2019).

5. ACKNOWLEDGEMENTS

The authors acknowledge CAPES for financial support through PROEX/CAPES program, and the National Supercomputing Center (CESUP-UFRGS) and the National Laboratory for Scientific Computing (SDumont supercomputer, LNCC/MCTI, Brazil) for providing computational resources for the calculations reported in this paper.

6. REFERENCES

Abramovich, G., 1963. *The theory of turbulent jets*. Ph.D. thesis, MIT Press, Massachusetts Institute of technology.

Amielh, M., Djeridane, T., Anselmet, F. and Fulachier, L., 1996. "Velocity near-field of variable density turbulent jets". *International Journal of Heat and mass transfer*, Vol. 39, No. 10, pp. 2149–2164.

Blazek, J., 2015. *Computational fluid dynamics: principles and applications*. Butterworth-Heinemann.

Brès, G.A. and Lele, S.K., 2019. "Modelling of jet noise: a perspective from large-eddy simulations". *Philosophical Transactions of the Royal Society A*, Vol. 377, No. 2159, p. 20190081.

Chen, C.J. and Rodi, W., 1980. "Vertical turbulent buoyant jets: a review of experimental data". *NASA Sti/Recon Technical Report A*, Vol. 80.

Deardorff, J.W., 1970. "A numerical study of three-dimensional turbulent channel flow at large reynolds numbers". *Journal of Fluid Mechanics*, Vol. 41, No. 2, pp. 453–480.

Djeridane, T., Amielh, M., Anselmet, F. and Fulachier, L., 1996. "Velocity turbulence properties in the near-field region of axisymmetric variable density jets". *Physics of Fluids*, Vol. 8, No. 6, pp. 1614–1630.

Ferziger, J.H. and Peric, M., 2012. *Computational methods for fluid dynamics*. Springer Science & Business Media.

Fortuna, A.d.O., 2000. *Técnicas computacionais para dinâminca dos fluidos: conceitos básicos e aplicações*. Edusp.

Hällqvist, T., 2006. *Large eddy simulation of impinging jets with heat transfer*. Ph.D. thesis, Royal Institute of Technology.

Hirt, C. *et al.*, 1975. "Sola: A numerical solution algorithm for transient fluid flows". Technical report, Los Alamos Scientific Lab., N. Mex.(USA).

Huai, Y., 2006. *Large Eddy Simulation in the scalar field*. Ph.D. thesis, Technische Universität.

Ilyushin, B. and Krasinsky, D., 2006. "Large eddy simulation of the turbulent round jet dynamics". *Thermophysics and Aeromechanics*, Vol. 13, No. 1, pp. 43–54.

Jones, S., Sotiropoulos, F. and Sale, M., 2002. "Large-eddy simulation of turbulent circular jet flows". Technical report, EERE Publication and Product Library, Washington, DC (United States).

Kuo, K.K.y. and Acharya, R., 2012. *Fundamentals of Turbulent and Multi-Phase Combustion*. John Wiley & Sons.

Lesieur, M., Métais, O. and Comte, P., 2005. *Large-eddy simulations of turbulence*. Cambridge University Press.

Lipari, G. and Stansby, P.K., 2011. "Review of experimental data on incompressible turbulent round jets". *Flow, turbulence and combustion*, Vol. 87, No. 1, pp. 79–114.

Markesteijn, A.P. and Karabasov, S.A., 2018. "GPU CABARET solutions for the cojen jet noise experiment". In *2018 AIAA/CEAS Aeroacoustics Conference*. p. 3921.

McMillan, O., 1980. "Tests of new subgrid-scale models in strained turbulence. aiaa paper aiaa-80-1339". In *AIAA 13th Fluid and Plasma Dynamics Conference, Snowmass, Co*.

Moin, P., Squires, K., Cabot, W. and Lee, S., 1991. "A dynamic subgrid-scale model for compressible turbulence and scalar transport". *Physics of Fluids A: Fluid Dynamics*, Vol. 3, No. 11, pp. 2746–2757.

Pinho, J. and Muniz, A.R., 2020. "PMLES: A hybrid openMP CUDA source code for LES of turbulent flows". *Journal of Applied Fluid Mechanics*, Vol. 13, No. 4, pp. 1067–1079.

Piomelli, U., 1999. "Large-eddy simulation: achievements and challenges". *Progress in Aerospace Sciences*, Vol. 35, No. 4, pp. 335–362.

Pope, S.B., 2000. *Turbulent flows*. Cambridge university press.

Quadros, A.E.R., 2016. *Processamento Paralelo em CUDA Aplicado ao Modelo de Geração de cenários sintéticos de vazões e Energias-GEVAZP*. Ph.D. thesis, Universidade Federal do Rio de Janeiro.

Ruetsch, G. and Fatica, M., 2011. "Cuda fortran for scientists and engineers". *NVIDIA Corporation*, Vol. 2701.

Sagaut, P., 2006. *Large eddy simulation for incompressible flows: an introduction*. Springer Science & Business Media.

Silva Freire, A.P., Menut, P.P.M. and Jian, S., 2002. *Turbulência*, Vol. 1. ABCM.

Smagorinsky, J., 1963. "General circulation experiments with the primitive equations: I. the basic experiment". *Monthly weather review*, Vol. 91, No. 3, pp. 99–164.

Terrana, S., Nguyen, C. and Peraire, J., 2020. "Gpu-accelerated large eddy simulation of hypersonic flows". In *AIAA Scitech 2020 Forum*. p. 1062.

Wang, P., Fröhlich, J., Michelassi, V. and Rodi, W., 2008. "Large-eddy simulation of variable-density turbulent axisymmetric jets". *International Journal of Heat and Fluid Flow*, Vol. 29, No. 3, pp. 654–664.

Wilson, R.V. and Demuren, A.O., 1997. *Numerical simulation of turbulent jets with rectangular cross-section*. 97. National Aeronautics and Space Administration, Langley Research Center.

Wilson, T. *et al.*, 1988. "Sola-dm: A numerical solution algorithm for transient three-dimensional flows". Technical

report, Los Alamos National Lab.

7. RESPONSIBILITY NOTICE

The following text, properly adapted to the number of authors, must be included in the last section of the paper: The author(s) is (are) solely responsible for the printed material included in this paper.